Tuning for robust and optimal dynamic positioning control in BlueROV2

Tuning for robust and optimal dynamic positioning control in BlueROV2

X Yang and Y Xing *

University of Stavanger, Norway

* Contact author: yihan.xing@uis.no

Abstract. A tuning approach for the robust and optimal dynamic positioning control of BlueROV2 subjected to currents with varying speeds and headings is presented. A 2D planar dynamic model of BlueROV2 is developed in Matlab/Simulink and used for the study. The surge, sway and yaw motions are controlled by individual PID controllers. An extensive sensitivity study is carried out on a total of nine cases with different current speeds, current headings, and measurement noise levels. The results show that tuning a model solely using step responses from a linearized model might not produce optimal results. Further it is important to verify the system responses in time domain after tuning. Finally, it is observed that re-tuning the controllers for each simulation case may lead to better performance. However, it is also shown that the base case controller gains are sufficiently robust and lead to good performances for the other simulation cases.

1. Introduction

There has been a general increase in interest in the study of underwater vehicles in recent years [1]. Underwater vehicles can be classified as remotely operated vehicles (ROVs) [2] and autonomous underwater vehicles (AUVs). These are commonly used in a wide range of underwater missions in many industries such aquaculture, defense, and oil and gas. A ROV is usually controlled by an operator on the ship or on shore via a tether and is used for a wide range of operations from inspection to intervention work. AUVs on the other hand operate independently underwater for longer periods of time and are normally utilized for inspection work. A brief comparison of the important features in ROV and AUV is presented in Table 1.

Table 1. Comparison between ROV and AUV

Feature	ROV	AUV
Controllability	More controllable; controlled remotely by operators	Without any manual intervention; controlled by a pre-set program
Working range	Limited due to tether length	No limitation
Ability	Multifunctional with different tools	Commonly with single function
Dynamics	Generally fully-actuated	Generally underactuated

Accurate, optimal and robust navigation is crucial for these vehicles to operate effectively underwater. During some operations, such as dynamic positioning [3], path tracking or target following, the ROV would also work like an AUV controlled by a pre-set program. In this paper, the authors will investigate the implementation of dynamic positioning in the BlueROV2 [4] as illustrated in Figure 1. BlueROV2 is a popular commercial mini ROV produced by Blue Robotics that is commonly used in scientific research. For example, BlueROV2 has been used as an imaging tool for the exploration of coral bleaching [5]. Although BlueROV2 is a tethered underwater vehicle, it still has the possibility to be easily modified into an autonomous vehicle due to its utilization of open-source software. This provides a fully featured open-source solution for ROVs and AUVs allowing the BlueROV2 to work with a wide variety of hardware such as sonar sensors, cameras, and an inertial navigation system. Autonomous capabilities can be implemented on the BlueROV2 with custom-written code utilizing this hardware. For example, Ludvigsen et al. [6] discussed the implementation of computer vision assisted navigation in BlueROV2. More details of BlueROV2 are presented in Section 2. .

Figure 1. BlueROV2 (base version)

A 2D planar model of the BlueROV2 is developed to study the dynamic positioning problem as illustrated in Figure 2 where the BlueROV2 is subjected to a Gaussian current coming in at an arbitrary Gaussian heading.

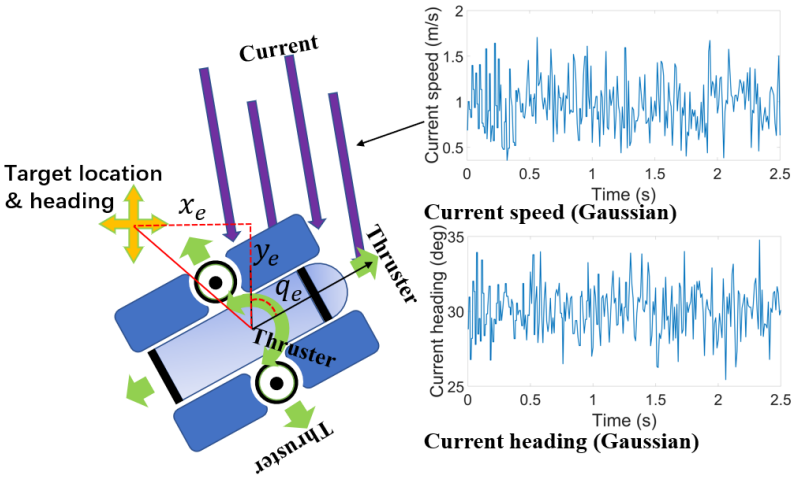

Figure 2. Dynamic positioning of BlueROV2 subjected to a current coming at an arbitrary heading

The dynamic positioning is controlled using proportional-integral-derivative (PID) control [7]. The PID tuner tool from Simulink [8] is used for the tuning of the controller gains. More details of the model and the tuners are provided in Section 3. . Even though a 2D planar problem using PID control is studied in this paper, the model can be easily extended to be a full 3D model and to use other more advanced control methods.

2. Description of BlueROV2

The BlueROV2 used in this paper and previously presented in Figure 1 is the base version offered by Blue Robotics. It is a mini observation class ROV that can operate up to 100 m. It is equipped with four horizontal and two vertical T200 thrusters which allow propulsion in 6 independent DOFs. The thruster configuration is presented in Figure 3.

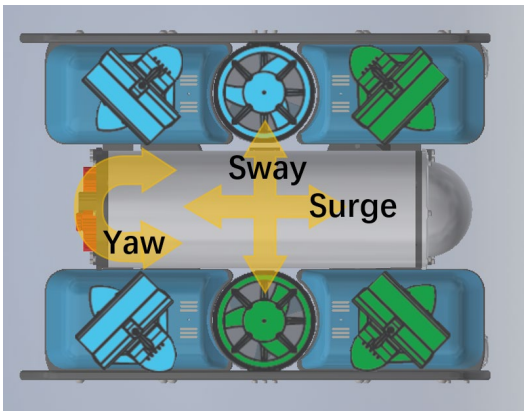

Figure 3. Thruster configuration of BlueROV2 from top view. Green and blue represent counterclockwise and clockwise propellers, respectively.

Table 2. Main BlueROV2 parameters

Parameters	Symbol	Value	Unit
Length	L	0.457	m
Width	W	0.338	m
Height	H	0.254	m
Mass	m	10.565	kg
Yaw moment	I_{zz}	0.201	kg·m
Surge added mass	I_{Ax}	10.565	kg
Sway added mass	I_{Ay}	10.565	kg
Yaw added mass	I_{An}	0.201	kg·m
Quadratic damping coefficient	C_D	0.5	-
Surge cross section area	A_x	0.048	m^2
Sway cross section area	A_y	0.10	m^2
Yaw cross section area	A_n	0.07	m^5

BlueROV2 is driven by the open-source Ardusub software [9] running on an open-source Pixhawk autopilot system [10]. The PixHawk autopilot is a powerful open-source hardware platform that has an

on-board inertia measurement unit and multiple I/O ports and has been adapted for use in a wide variety of drones (air/land/sea). The Raspberry Pi 3 [11] is used as a companion computer to provide HD video streaming to the surface workstation via the tether and Fathom X interface [12]. The main BlueROV2 parameters are presented in Table 2.

3. Theory

As mentioned, this paper will focus on 2D planar dynamics, i.e., only x-y plane motions are considered and there is no heave, roll and pitch motions. In addition, the following assumptions are made:

- The BlueROV2 is assumed to be hydrodynamically symmetrical, i.e., there are no hydrodynamic coupling terms.
- The BlueROV2 is assumed to operate far away from the wave-affected zone, i.e., the load-effects of waves are negligible and only currents will be considered.

3.1. Equations of motion

The equations of motions for a ROV can be described by the Newton-Euler equation as presented by Fossen [13]:

$$M\dot{v} + C(v)v + D(v)v + g(\eta) = \tau \quad (1)$$

where M is the mass matrix, $C(v)$ is the Coriolis matrix, $D(v)$ is the damping matrix, $g(\eta)$ is the gravitational forces and moments, v is the velocity and τ is the external driving forces.

For a 2D x-y planar dynamic problem solved in a global earth frame at a fixed latitude, $C(v)$ and $g(\eta)$ are zero and equation. (1) can be simplified and expanded to:

$$\begin{bmatrix} m + I_{Ax} & 0 & 0 \\ 0 & m + I_{Ay} & 0 \\ 0 & 0 & I_{zz} + I_{An} \end{bmatrix} \begin{bmatrix} \dot{u} \\ \dot{v} \\ \dot{w} \end{bmatrix} + \frac{1}{2}\rho C_D A \begin{bmatrix} |u| \\ |v| \\ |w| \end{bmatrix} \cdot \begin{bmatrix} u \\ v \\ w \end{bmatrix} = \begin{bmatrix} X \\ Y \\ T \end{bmatrix} \quad (2)$$

where $[u\ v\ w]^T$ are the velocities in surge, sway, yaw respectively, $[u\_dot\ v\_dot\ w\_dot]^T$ are the accelerations in surge, sway, yaw respectively and $[X\ Y\ T]^T$ are forces and moment in surge, sway, yaw. $[I_{Ax}\ I_{Ay}\ I_{An}]$ are added mass components, ρ is the density of water, C_D is the drag coefficient and A is the cross-section area for drag. Added mass on a rigid body is a virtual mass caused by the fluid around. In this study, added mass $[I_{Ax}\ I_{Ay}\ I_{An}]$ are assumed to be the same as the mass and inertia moment of BlueROV2 as listed in Table 2.

Based on the assumption of hydrodynamic symmetry, all coupled terms are not considered. Correspondingly, the drag force can be regarded to be proportional to the square of the relative velocity between current and act in the opposite direction to the ROV's motion. Given the above, drag forces in surge, sway and yaw can be expressed respectively as:

$$X_D = -\frac{1}{2}\rho C_D A_x |u| u \quad (3)$$

$$Y_D = -\frac{1}{2}\rho C_D A_y |v| v \quad (4)$$

$$\psi_D = -\frac{1}{2}\rho C_D A_n |w| w \quad (5)$$

The drag coefficients for three DOFs are all assumed to be 0.5 in this study. The cross-section areas for each direction are listed in Table 2.

3.2. Proportional-integral-derivative control

PID control is commonly adopted in unmanned underwater vehicles and marine operation field [14]. Two types of PID controllers are considered in this paper. One is a general PID controller that uses fixed controller gain values while the other one is a re-tuned PID controller which can adapt the controller gains for different scenarios.

Using the PID controller, the open-loop BlueROV2 control system can be transformed to a closed-loop control as shown in Figure 4. There are three PID controllers used, one for each individual direction, i.e., surge, sway and yaw.

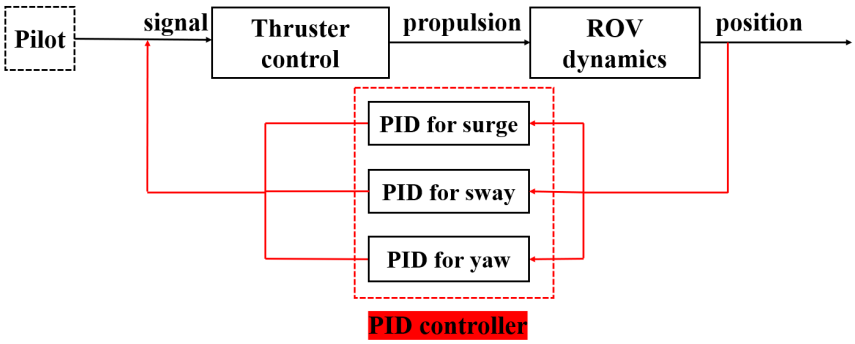

Figure 4. From open-loop control system to closed-loop control system with PID controller.

The input for a PID controller is the error *e(t)* between the measured process variable and the desired setpoint. The output *u(t)* is produced with a correction multiplied by a proportional gain (K_P), integral of the correction multiplied by an integral gain (K_I) and derivative of the correction multiplied by a derivative gain (K_D). The overall function of PID controller is given below:

$$u(t) = K_p e(t) + K_i \int_0^t e(t)\,dt + K_d \frac{de(t)}{dt} \quad (6)$$

In this study, *e(t)* is the errors [x_e y_e q_e] between the measured position of BlueROV2 [x_m y_m q_m] and coordinate of the desired point [x_t y_t q_t]. The output is the thruster forces signal [F_x' F_y' T_q'] used to control the BlueROV2 to approach the target. Since the input and output in this control system are both 3-dimensional, and each two of three components are uncoupled. As mentioned above, the PID controller used in is decentralized into 3 sub-PID controller for x_e & F_x', y_e & F_y' and q_e & T_q', respectively. Tuning this ROV motion control system involves the controller gains of individual PID controllers in surge, sway and yaw, i.e., their corresponding K_p, K_i and K_d values. As mentioned, two tuning methods are investigated in this paper. The first tuning method involves using a single set of K_p, K_i and K_d values for the whole system running process after proper tuning. The second tuning method uses K_p, K_i and K_d values that are retuned for each load case. In this way the control gains can be in theory adapted to different types of environmental loads and noise levels.

3.3. Tuning and desired system performance

The tuning tool used in this study is the Matlab PID tuner. The principle of the tuning method is discussed in Åström el al. [15]. The PID tuner uses a system model linearized at an operating point for tuning. By changing the Bandwidth and Phase margin setting in frequency domain, the tuner will derive the corresponding controller gains automatically and plot out the system impulse response. In this study,

rise time (T_{rise}), setting time ($T_{setting}$), percentage overshoot (PO) and gain margin (γ) are used performance indicators. These are briefly discussed in the following and presented in Figure 5.

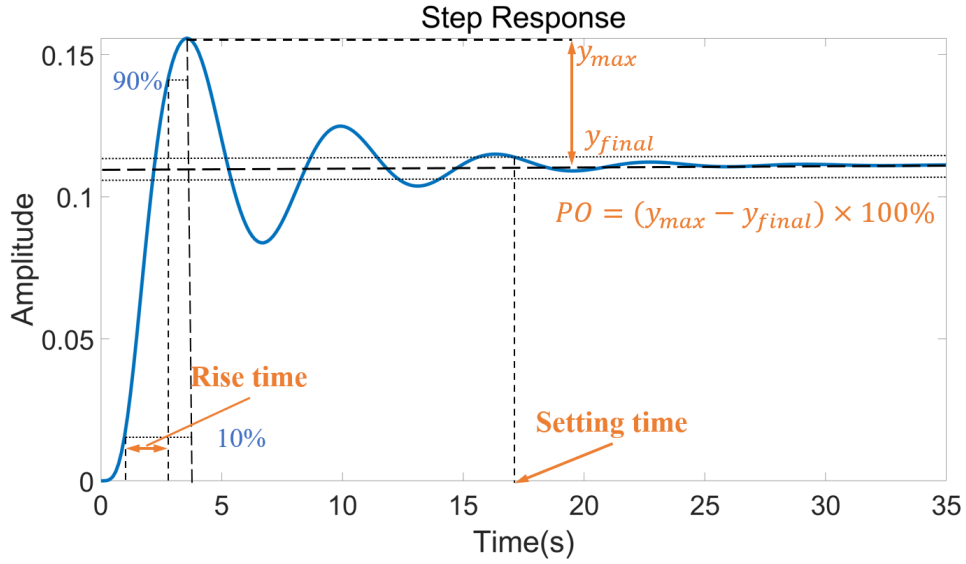

Figure 5. Rise time, setting time and overshoot

Rise time is defined as the time for the system to rise from 10% to 90% of the steady state value. Rise time represents the respond speed of the system. It is desired to have a quick response, i.e., below 3 seconds for the BlueROV2. Setting time of a system is the time it takes for the error *e(t)* to fall below 2% of the peak value of *e(t)*. A setting time reflects the ability of the system to stabilized. It is desired that the settling time of the BlueROV2 be less than 50 seconds. Percentage overshoot in a control system is the percentage of the maximum peak value of the response exceeding the final, steady-state value as expressed in equation (7). A larger overshoot represents more potential oscillation or less stability. It is desired to have an overshoot below 50% in this study. The gain margin is the difference between 0 dB and the gain at the phase-cross-over frequency which is at the phase equals to -180 degree. A larger gain margin means a more stable system. When the gain margin becomes negative, the system is unstable. Gain margins in the interval of [5 ,30] dB is desired for the BlueROV2.

$$PO = (y_{max} - y_{final}) \times 100\% \quad (7)$$

The base case in this paper has the following two sets of tuning objectives:

- Balanced - rise time < 1.5 s, setting time < 30 s, percentage overshoot < 30 % and gain margin > 5 dB.
- Rapid-response - rise time < 1 s, setting time < 10 s.

4. Simulink implementation

The Simulink implementation is illustrated in Figure 6.

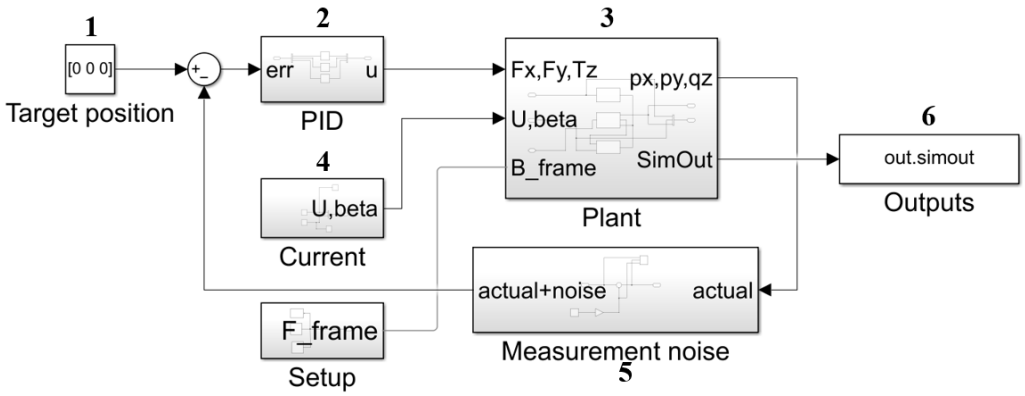

Figure 6. Simulink model diagram

The model consists of the following main blocks as labelled in Figure 6:

- Block 1: Provides the coordinates of the set location (x_{set}, y_{set}, z_{set}).
- Block 2: Contains the PID controllers. Each individual variable has an independent PID controller, i.e., a de-coupled PID control method is used.
- Block 3: Contains the plant model which considers the 2D planar dynamics of the BlueROV2.
- Block 4: Provides the gaussian current speeds and directions, and the global model set-up parameters.
- Block 5: Adds measurement noise into the ROV displacements measured from the plant model (Block 3).
- Block 6: Stores the simulation outputs.

4.1. Plant model

The plant model (Block 3 in Figure 6) is presented in more details in this sub-section. A zoom view into the plant model is presented in Figure 7.

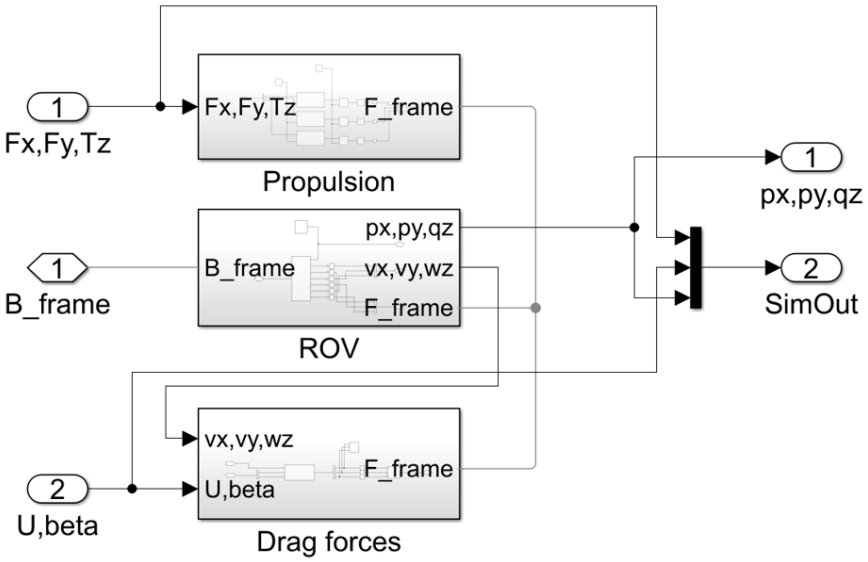

Figure 7. Plant model diagram

The plant model consists of three main blocks:

- Propulsion: This block models the propulsion forces. The block takes in the commanded forces and torque (F_x, F_y and T_z) as inputs and applies them to the ROV block. To remove high frequency noise, a low pass filter with cut-off frequency of 1 Hz is also applied on the commanded signals before they are used as forces and torque. The forward and lateral thrust forces are saturated to [-88.3 ,88.3] N and the yaw moment is saturated to [-17.5 ,17.5] N·m in accordance with the physical limitations of the T200 thrusters.
- ROV: This block contains a 2D planar rigid body with 3 degrees of freedom (x, y and w). Simulink will solve the equation of motion in accordance with equation (2) based on the forces and torque applied to the rigid body.
- Drag forces: This block calculates the drag forces and torque based on the current speed and ROV's velocities in accordance with equations (3), (4) and (5) and then applies them to the ROV block.

5. Case studies

To explore the effect of tuning, several cases with different current speeds, headings, coefficients of variation (c_V) and measurement noise levels presented in Table 3 are considered.

Table 3. Simulation cases

Case name	Current speed	Current heading	c_V	Control type	Noise
1-30-0.1-fx-lv1	1 m/s	30 deg	0.1	fixed	Level 1
1.5-30-0.1-fx-lv1	1.5 m/s	30 deg	0.1	fixed	Level 1
1-45-0.1-fx-lv1	1 m/s	45 deg	0.1	fixed	Level 1
1-30-0.15-fx-lv1	1 m/s	30 deg	0.15	fixed	Level 1
1-30-0.1-fx-lv2	1 m/s	30 deg	0.1	fixed	Level 2
1.5-30-0.1-tn-lv1	1.5 m/s	30 deg	0.1	tuned	Level 1
1-45-0.1-tn-lv1	1 m/s	45 deg	0.1	tuned	Level 1
1-30-0.15-tn-lv1	1 m/s	30 deg	0.15	tuned	Level 1
1-30-0.1-tn-lv2	1 m/s	30 deg	0.1	tuned	Level 2

The first case, i.e., 1-30-0.1-fx-lv1 is the base case. 'fixed' mean that the parameters K_p, K_i, K_d and filter coefficient N are fixed as the same as those tuned in the base case. 'tuned' means K_p, K_i, K_d and N are retuned to adapt to the current case. The objective in the retuning is to readjust the bandwidth and phase margin back to the same values as in the base case. Level 1 means that the gain for noise in surge direction = 0.001, gain for noise in sway direction = 0.001 and gain for noise in yaw motion = 0.00001. Level 2 means that the gain for noise in surge direction = 0.002, gain for noise in sway direction = 0.002 and gain for noise in yaw motion = 0.00002.

6. Results and discussions

6.1. Base case gains

The controller gains for the Base Case (1-30-0.1-fx-lv1) are presented in **Error! Reference source not found.** and **Error! Reference source not found.** when balanced tuning and rapid-response tuning approaches are used, respectively. The tuning objectives were previously discussed in Section 3.3. .

Table 4. PID gains for Base Case with balanced tuning

	K_p	K_i	K_d	N
Surge	3.4619	0.0275	21.157	109.48
Sway	10.901	0.7667	20.531	100.06
Yaw	0.0084	0.000043	0.3632	100.52

Table 5. PID gains for Base Case with rapid response tuning

	K_p	K_i	K_d	N
Surge	14.936	0.1468	21.752	130.32
Sway	26.426	7.6454	22.681	118.54
Yaw	0.1260	0.00125	0.4818	135.08

A comparison of the time series of the x-position, y-position and heading angle when balanced and rapid-response tuning approaches are used is presented in Figure 8. As observed, the rapid-response approach leads to a faster system response; the orange line tends to lead the blue line in Figure 8. This effect is particularly pronounced in the heading angle response.

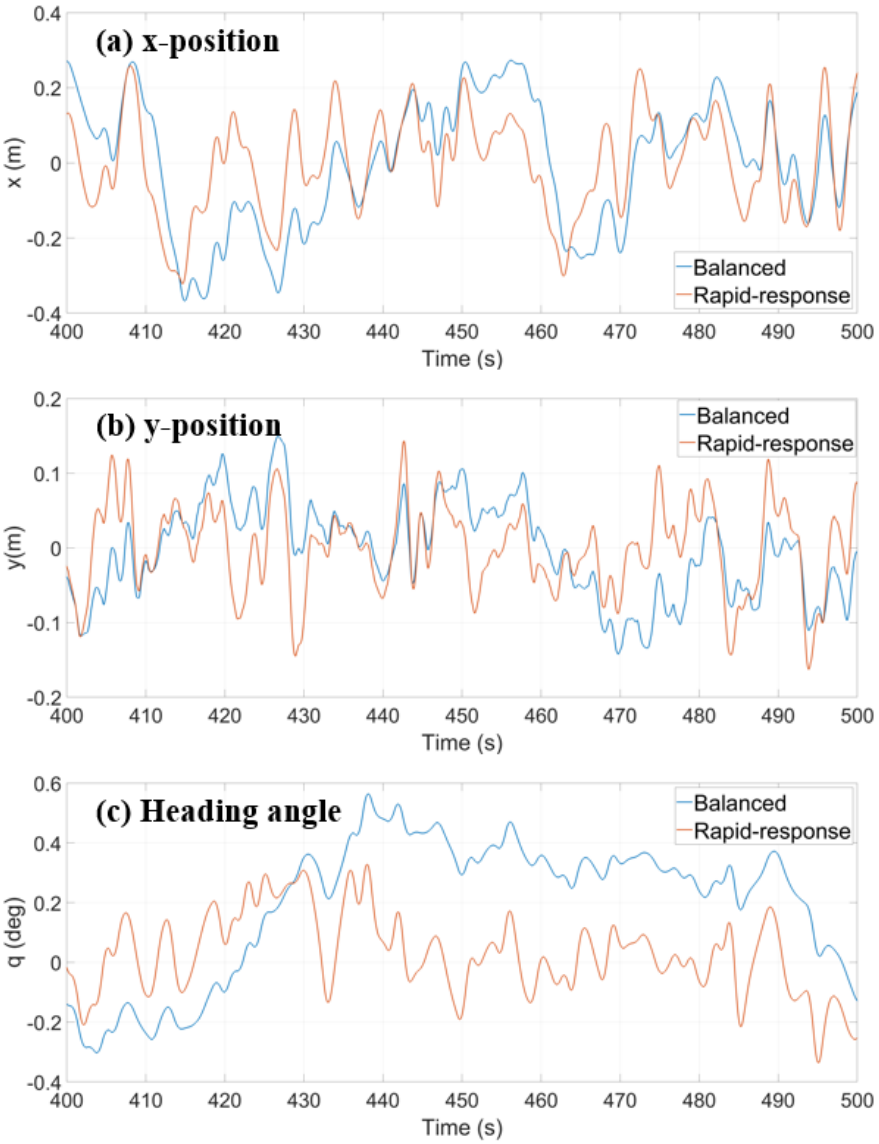

Figure 8. Time series of (a) x-position, (b) y-position, (c) heading angle, Base case, 1-30-0.1-fx-lv1, Balanced vs Rapid-response tuning approach.

6.2. Sensitivity study performed on Base Case

A sensitivity study is performed on the base case (1-30-0.1-fx-lv1) to explore the relationship between controller gains and performance in term of rise time, settling time, overshoot and gain margin. The study is performed on a model linearised at t = 450 s. The surge (x-dir) component is presented. The results are presented in Figure 9, Figure 10, Figure 11 and Figure 12 for rise time, settling time, overshoot and gain margin, respectively.

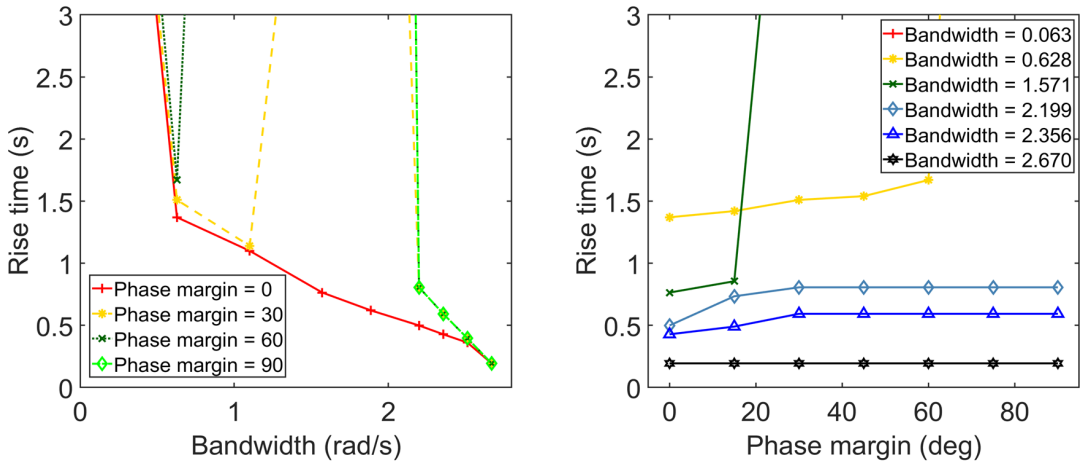

Figure 9. Base Case (1-30-0.1-fx-lv1), Surge (x-dir), Rise Time vs Bandwith and Phase Margin

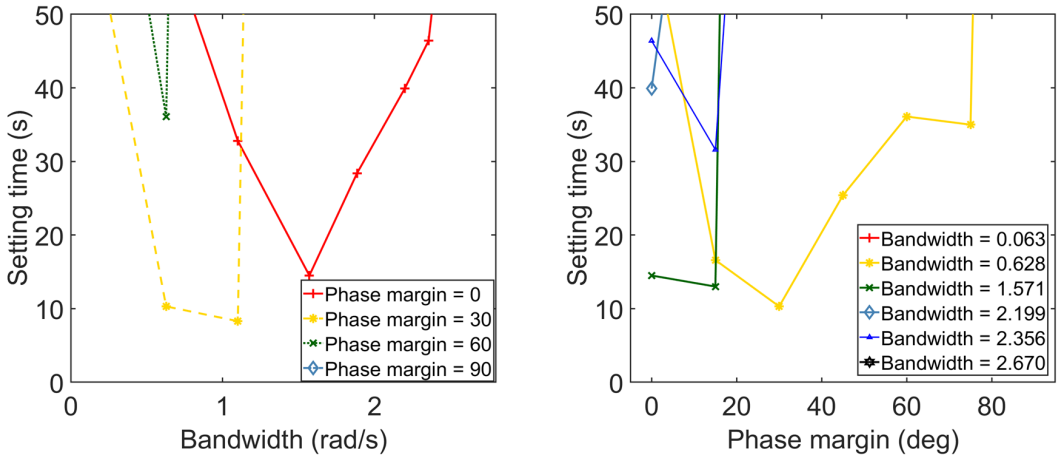

Figure 10. Base Case (1-30-0.1-fx-lv1), Surge (x-dir), Settling Time vs Bandwith and Phase Margin

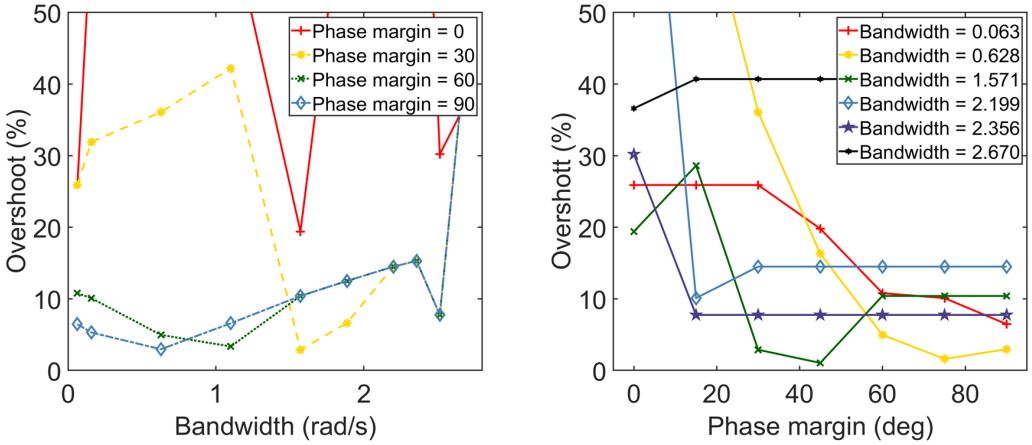

Figure 11. Base Case (1-30-0.1-fx-lv1), Surge (x-dir), Overshoot vs Bandwith and Phase Margin

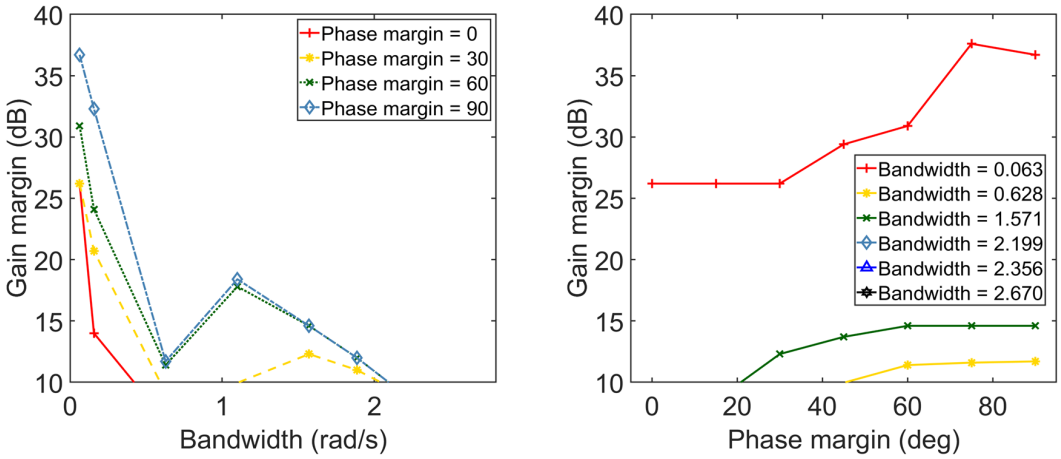

Figure 12. Base Case (1-30-0.1-fx-lv1), Surge (x-dir), Gain Margin vs Bandwith and Phase Margin

The following observations are made:

- Rise time decreases rapidly with increasing bandwidth but is not affected by changes in phase margin.
- Settling time has a concave relationship (decreases then increases) with increasing bandwidth and phase margin.
- Overshoot is not affected by changes in bandwidth but decreases with increasing phase margin.
- Gain margin decreases with increasing values of bandwidth increasing but is not affected by changes in phase margin.

The above observations provide guidance for the subsequent controller tuning process that is performed in this paper.

6.3. Parametric correlation analysis

A parametric correlation analysis is performed to quantify the relationship between controller gains and performance variables. From the sensitivity study performed in Section 6.1. , it is evident that the relationships between these are nonlinear. Therefore, a determination matrix which quantifies quadratic correlations is computed. The coefficient of determination, r^2 that relates variables x and y is expressed as:

$$r^2 = \frac{\sum(y_i - \bar{y})^2 - \frac{n-1}{n-2}(y_i - Y_i)^2}{\sum(y_i - \bar{y})^2} \quad (8)$$

where n is the total number of samples and $Y_i = ax_i^2 + bx_i + c$. The coefficient of determination has a value of 0 to 1. A value of 0 means no correlation, while a value of 1 means perfect correlation. The determination matrix is presented in Figure 13.

	Bandwidth	Phase margin	Rise time	Settling time	Overshoot	Gain margin	Kp	Ki	Kd
Bandwidth	1.00	0.00	0.22	0.01	0.01	0.66	0.16	0.10	0.16
Phase margin	0.00	1.00	0.22	0.20	0.48	0.10	0.47	0.42	0.00
Rise time	0.44	0.21	1.00	0.28	0.15	0.65	0.16	0.08	0.37
Settling time	0.05	0.34	0.35	1.00	0.27	0.07	0.24	0.27	0.13
Overshoot	0.00	0.40	0.17	0.27	1.00	0.14	0.23	0.23	0.03
Gain margin	0.64	0.10	0.34	0.08	0.19	1.00	0.21	0.16	0.53
Kp	0.14	0.39	0.14	0.07	0.22	0.28	1.00	0.63	0.57
Ki	0.03	0.33	0.07	0.08	0.25	0.13	0.71	1.00	0.00
Kd	0.97	0.01	0.17	0.01	0.04	0.51	0.10	0.04	1.00

Figure 13. Determination matrix

The following observations are made:

- Rise time has an inverse quadratic coefficient of determination of 0.44 which means it has a somewhat quadratic relationship with bandwidth.
- The quadratic coefficients of determination between setting time and phase margin are 0.28 and 0.34 (inverse). This means a slight correlation.
- Percentage overshoot has quadratic coefficients of determination of 0.48 and 0.40 (inverse) with phase margin which means they are fairly correlated.
- The quadratic coefficients of determination between gain margin and bandwidth are 0.66 and 0.64 (inverse) which indicates a relatively strong correlation.

The observations are summarized in Table 6. '+' indicates improved performance, '–' indicates impaired performance and '0' indicates no clear trend.

Table 6. Summary of observations from determination matrix

Performance variable	Bandwidth	Phase margin
T_{rise}	++	0
$T_{settling}$	+-	+-
PO	0	++
γ	-	0

6.4. Different simulation cases

The other different simulation cases presented in Table 3 are studied in this sub-section using controller gains derived from both balanced and rapid-response approaches.

6.4.1. Step responses using Base Case gains. The system step responses when base case gains are used are presented in Figure 14 and Figure 15 for the balanced and rapid-response tuning approaches, respectively.

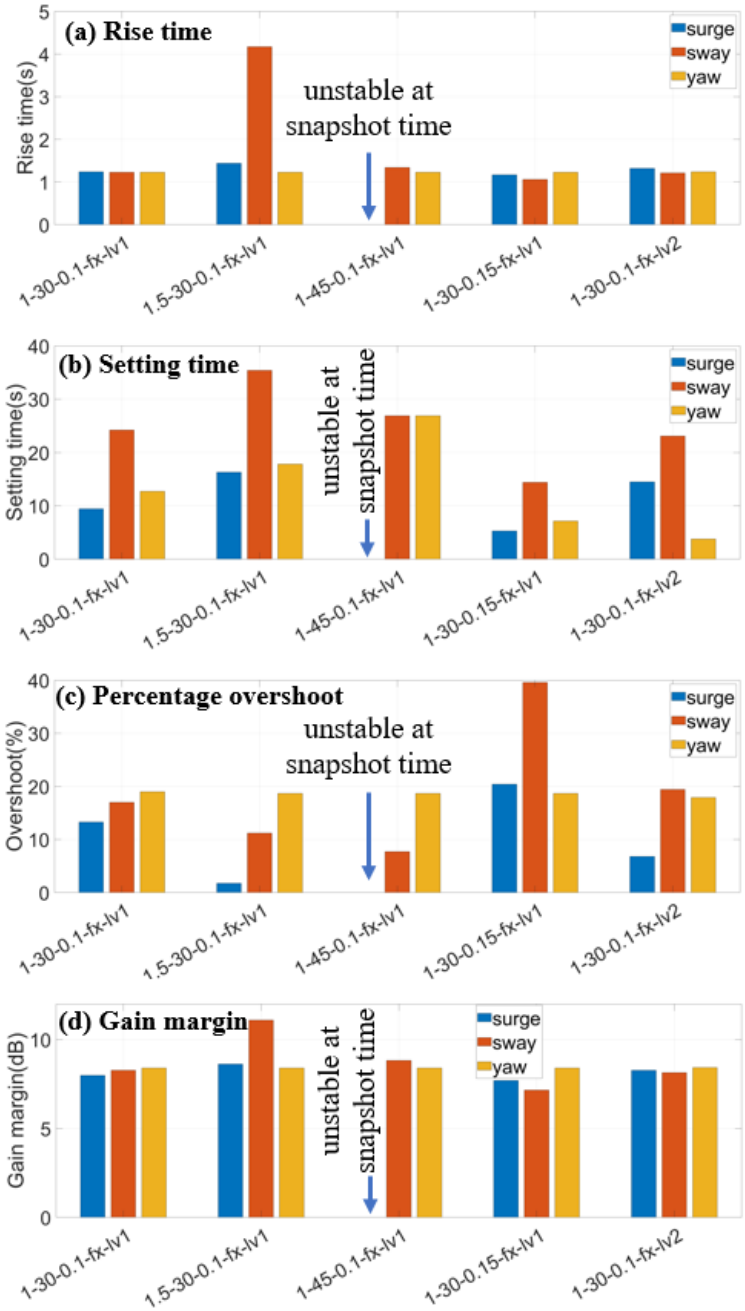

Figure 14. Balanced tuning approach, Step responses for different simulation cases, (a) Rise time, (b) Setting time, (c) Percentage overshoot and (d) Gain margin

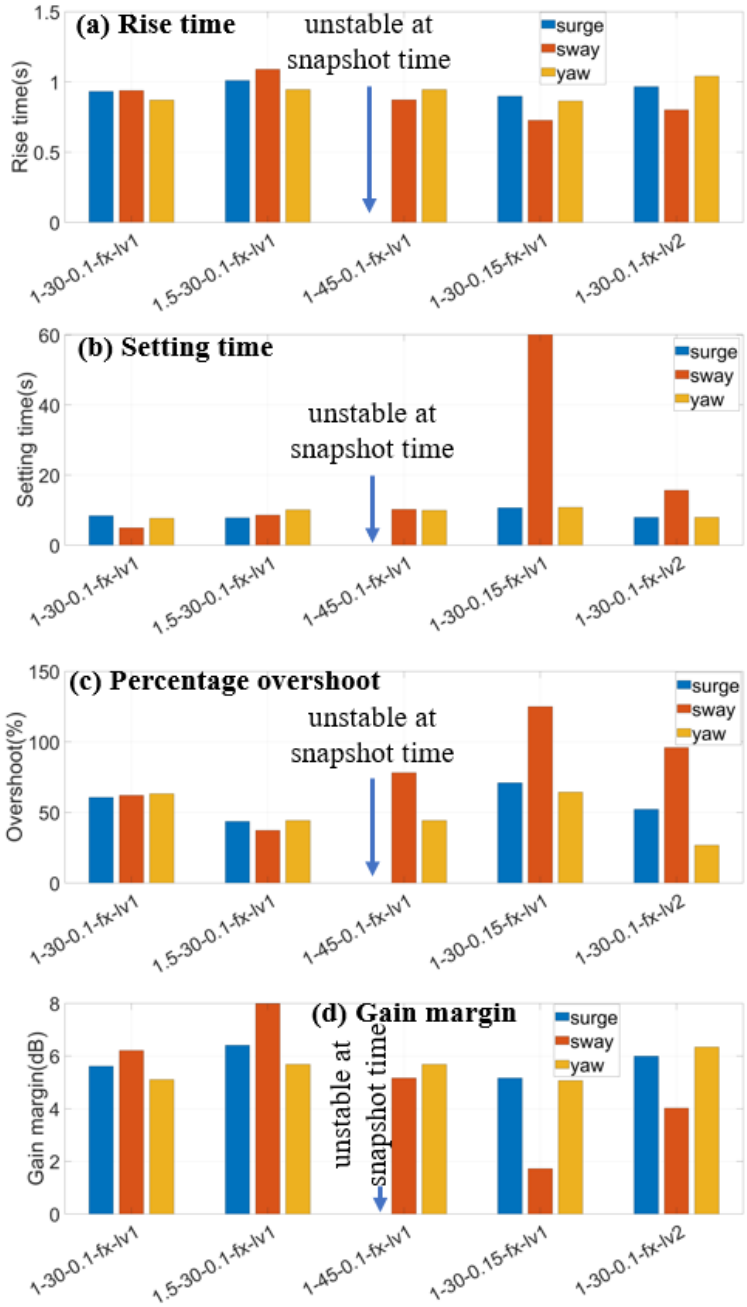

Figure 15. Rapid-response tuning approach, Step responses for different simulation cases, (a) Rise time, (b) Setting time, (c) Percentage overshoot and (d) Gain margin

In general, it is observed that the step responses are in general similar for the different cases except for the following cases:

- Surge component in 1-45-0.1-fx-lv1 and 1-45-0.1-tn-lv1: The system is unstable under a current heading of 45 degree.
- Sway component in 1.5-30-0.1-fx-lv1: The rise time increases when the balanced tuning approach is used.
- Sway component in 1-30-0.15-fx-lv1: The settling time becomes as large as 60 seconds when the rapid-response tuning approach is used.

To explore how these exceptions will affect the BlueROV2's performance, the time series of responses will be shown and discussed in the following sub-section.

6.4.2. Time series of responses. The time series of the corresponding responses of the cases presented in Figure 14 and Figure 15 are presented in Figure 16, Figure 17 and Figure 18 for the x-position, y-position and heading, respectively.

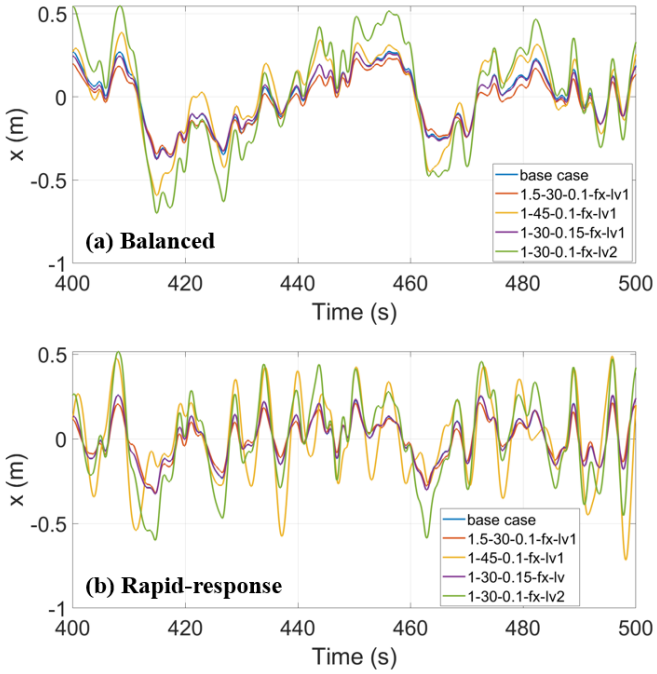

Figure 16. x-position for different simulation cases, (a) Balanced tuning, (b) Rapid-response tuning

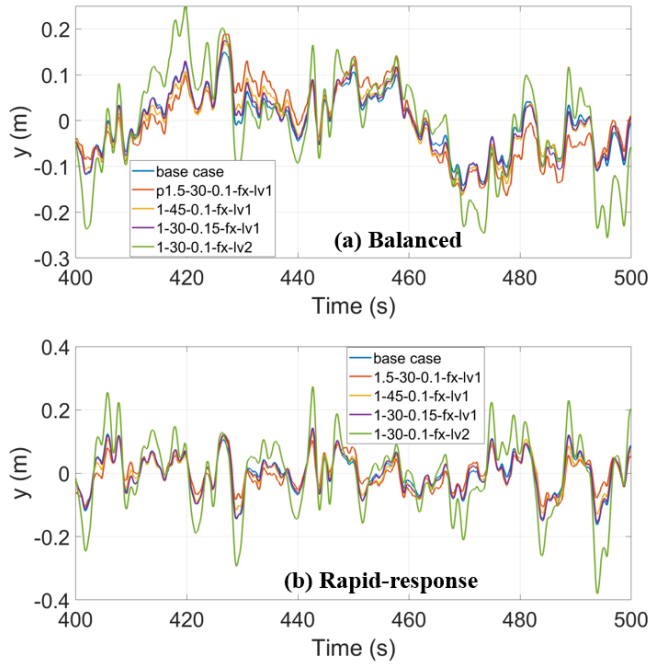

Figure 17. y-position for different simulation cases, (a) Balanced tuning, (b) Rapid-response tuning

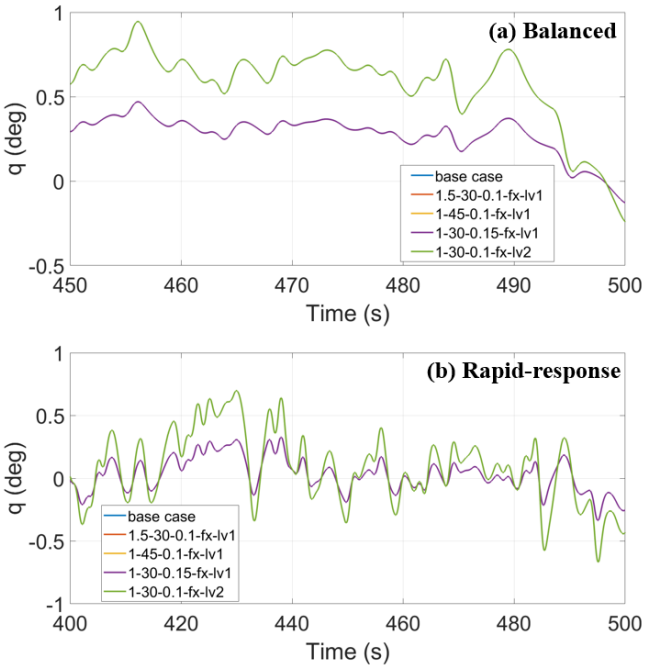

Figure 18. Heading for different simulation cases, (a) Balanced tuning, (b) Rapid-response tuning

In general, actual time domain responses show larger differences between the different simulation cases compared to that observed from the step responses presented in Section 6.4.1. . This means that it is important not to rely on the step responses purely and excessively when tuning is performed. It is important to always test the system out in time domain and observe the actual time domain responses. It is also observed that the rapid-response tuning approach produces a somewhat poorer performance compared to the balanced tuning approach.

6.4.3. Effect of re-tuning. In this section, improvements will be attempted on the time domain performances presented in Section 6.4.2. by performing re-turning for each simulation case. The time domain responses are presented in Figure 19, Figure 20 and **Figure 21**, respectively for heading, x-position and y-position. In general, it is observed that re-tuning the PID controllers leads to better performances.

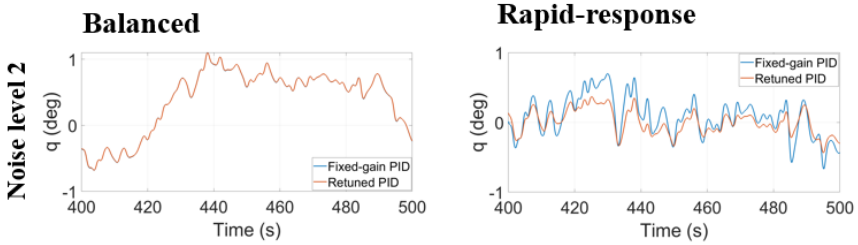

Figure 19. Comparison of responses from using fixed gains vs retuned gains, heading

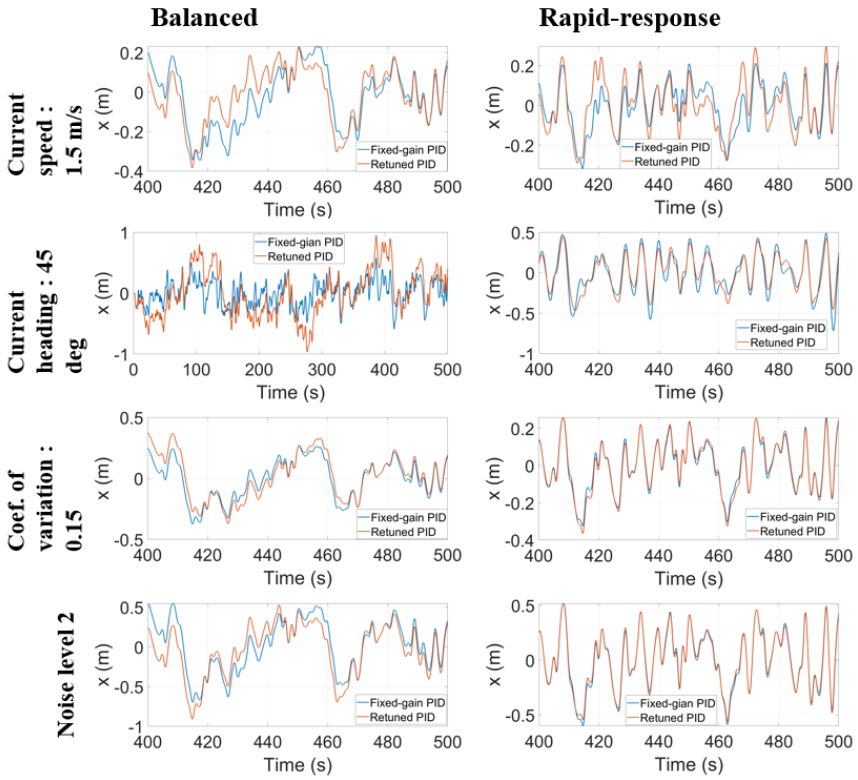

Figure 20. Comparison of responses from using fixed gains vs retuned gains, x-position

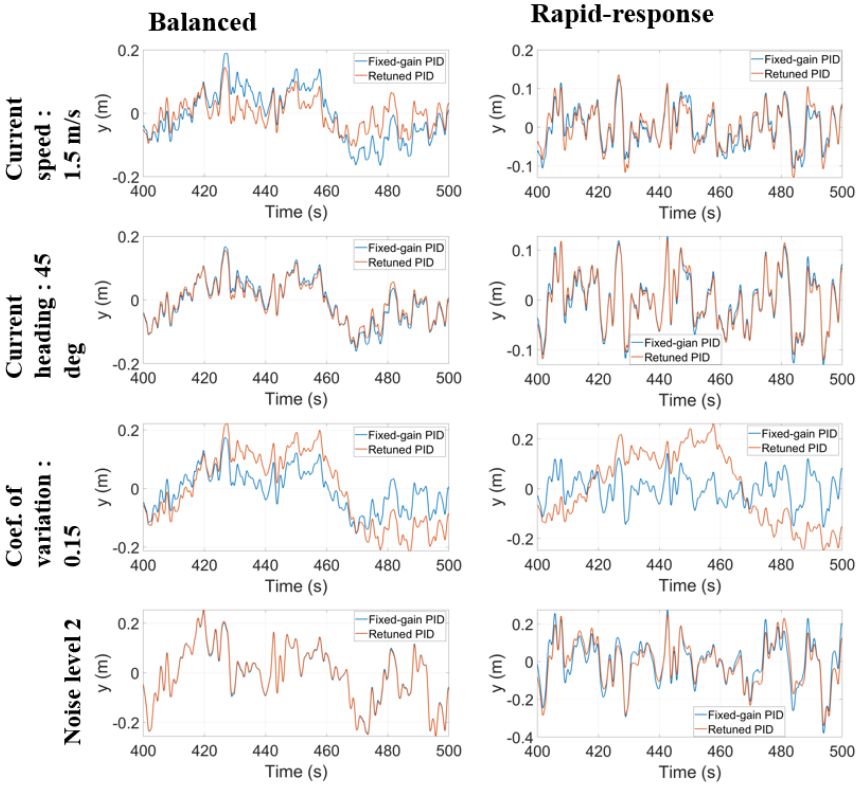

Figure 21. Comparison of responses from using fixed gains vs retuned gains, y-position

7. Conclusions

In this paper, a tuning approach for the robust and optimal dynamic positioning control of BlueROV2 subjected to currents with varying speeds and headings is presented. The results show that tuning a model solely using step responses from a linearized model might not produce optimal results. Further it is important to verify the system responses in time domain after tuning. Finally, it is observed that re-tuning the controllers for each simulation case may lead to better performance. However, it is also shown that the base case controller gains are sufficiently robust and lead to good performances for the other simulation cases.

References

[1] Wu C J 2018 *6-DoF Modelling and Control of a Remotely Operated Vehicle* (Flinders University: Masters thesis).
[2] Christ R D and Wernli R L 2014 *The ROV Mannual: a User Guide for Remotely Operated Vehicles 2nd Ed.* (Oxford: Elsevier).
[3] Sørensen A J 2011 A survey of dynamic positioning control systems, *Annu. Rev. Control* **35**(1), 123-136.
[4] Blue Robotoics 2021 *BlueROV2 Datasheet*.
[5] Teague J, Willans J, Allen M J, Scott T and Day J C 2019 Applied marine hyperspectral imaging; Coral Bleaching from a spectral viewpoint. *Spectrosc. Eur.* **31**, 13–17
[6] Ludvigsen M, Johnsen G, Sørensen A J, Lågstad P A and Ødegård Ø 2014 Scientific operations combining ROV and AUV in the Trondheim Fjord, *Mar. Technol. Soc. J.* **48**(2), 59-71
[7] Johnson M A and Moradi M H 2005 *PID Control: New Identification and Design Methods* (London: Springer).
[8] MathWorks 2021 *Simulink*. Assessed 27.06.2021 from https://se.mathworks.com/products/simulink.html
[9] Blue Robotics 2017 *ArduSub Project*. Assessed 27.06.2021 from https://www.ardusub.com/
[10] Meier L 2021 *Official Pixhawk Website*. Assessed 27.06.2021 from https://pixhawk.org/
[11] Raspberry Pi Foundation 2021 *Raspberry Pi 3 Model B*. Assessed 27.06.2021 from https://www.raspberrypi.org/products/raspberry-pi-3-model-b/
[12] Blue Robotics 2021 *Fathom-X Tether Interface Board Set*. Assesed 27.06.2021 from https://bluerobotics.com/store/comm-control-power/tether-interface/fathom-x-r1/
[13] Fossen T I 2011 *Handbook of Marine Craft Hydrodynamics and Motion Control* (West Sussex: John Wiley & Sons).
[14] Schjølberg I and Utne I B 2015 Towards autonomy in ROV operations, *IFAC J. Syst. Control* **48**(2), 183-188.
[15] Åström K J and Hägglund T 2006 *Advanced PID Control* (ISA - The Instrumentation, Systems and Automation Society).